Mechanics of Advanced Materials and Structures
Publication details, including instructions for authors and subscription information:
http://www.tandfonline.com/loi/umcm20

Adaptive Methods for Analysis of Composite Plates with Radial Basis Functions

A. M. A. Neves [a], T. A. Driscoll [b], A. R. H. Heryudono [b], A. J. M. Ferreira [a], C. M. M. Soares [c] & R. M. N. Jorge [a]

[a] Departamento de Engenharia Mecâânica e Gestãão Industrial, Faculdade de Engenharia da Universidade do Porto, Rua Dr. Roberto Frias, Porto, Portugal

[b] Department of Mathematical Sciences, University of Delaware, Newark, Delaware, USA

[c] IDMEC——Instituto de Engenharia Mecâânica——Instituto Superior Téécnico, Av. Rovisco Pais, 1096, Lisboa Codex, Portugal

Available online: 08 Sep 2011

To cite this article: A. M. A. Neves, T. A. Driscoll, A. R. H. Heryudono, A. J. M. Ferreira, C. M. M. Soares & R. M. N. Jorge (2011): Adaptive Methods for Analysis of Composite Plates with Radial Basis Functions, Mechanics of Advanced Materials and Structures, 18:6, 420-430

To link to this article: http://dx.doi.org/10.1080/15376494.2010.528155

Mechanics of Advanced Materials and Structures, 18:420–430, 2011

ISSN: 1537-6494 print / 1537-6532 online
DOI: 10.1080/15376494.2010.528155

Taylor & Francis
Taylor & Francis Group

Adaptive Methods for Analysis of Composite Plates with Radial Basis Functions

A. M. A. Neves,[1] T. A. Driscoll,[2] A. R. H. Heryudono,[2] A. J. M. Ferreira,[1] C. M. M. Soares,[3] and R. M. N. Jorge[1]

[1]*Departamento de Engenharia Mecânica e Gestão Industrial, Faculdade de Engenharia da Universidade do Porto, Rua Dr. Roberto Frias, Porto, Portugal*
[2]*Department of Mathematical Sciences, University of Delaware, Newark, Delaware, USA*
[3]*IDMEC—Instituto de Engenharia Mecânica—Instituto Superior Técnico, Av. Rovisco Pais, 1096 Lisboa Codex, Portugal*

Driscoll and Heryudono [1] developed an adaptive method for radial basis functions method. This article addresses the adaptive analysis of composite plates in bending with radial basis multiquadric functions using Driscoll and Heryudono's technique. In this article, various laminates, thickness to side length ratios, and boundary conditions are considered. The method allows for a more natural and automatic selection of the problem grid, where the user must only define the error tolerance. The results obtained show an interesting and promising approach to the static analysis of composite laminates.

Keywords radial basis functions, adaptive methods, composite, plates, residual, subsampling, multiquadric

1. INTRODUCTION

Radial basis function (RBF) methods are a good alternative method for the numerical solution of partial differential equations (PDEs) [2–6]. Compared to low-order methods, such as finite differences, finite volumes, and finite elements, RBF-based methods offer numerous advantages, such as mesh-free discretization and simple implementation. The imposition of the essential and natural boundary conditions is straightforward.

Also, depending on how the RBFs are chosen, high-order or spectral convergence can be achieved [7].

For the application of fixed-grid RBF methods to laminated composite beams and plates, readers should consult [8–10].

Adaptive methods may be preferred over fixed grid methods in problems that exhibit high degrees of localizations such as steep gradients or corners. The goal is to obtain a numerical solution such that the error is below a prescribed accuracy with the smallest number of degrees of freedom. Since RBF methods are completely meshfree, requiring only interpolation nodes and a set of points called centers defining the basis functions, implementing adaptivity in terms of refining and coarsening nodes is straightforward. Driscoll and Heryudono [1] developed an adaptive algorithm for RBFs where results obtained on interpolation, boundary-value, and time-dependent problems are encouraging.

In the present work, we apply the residual subsampling technique developed by Driscoll and Heryudono to the static analysis of isotropic and symmetric laminated composite plates.

We considered the First Order-Shear Deformation Theory (FSDT) [11].

The method starts with nonoverlapping boxes, each containing an active center. Once an interpolant has been computed for the active center set, the residual of the resulting approximation is sampled on a finer node set in each box. Nodes from the finer set are added to or removed from the set of centers based on the size of the residual of the PDE at those points. The interpolant is then recomputed using the new active center set for a new approximation.

We organize the article as follows. In Section 2 we review the governing differential equations for the bending of laminated plates using the FSDT. The RBF implementation is shortly reviewed in Section 3. In Section 4 we explain in detail the application of the residual subsampling technique to plates. Numerical results for isotropic and composite square plates are presented in subsections 5.1 and 5.2, respectively, and discussed in subsections 5.3. Finally some conclusions are presented in Section 6.

2. ANALYSIS OF SYMMETRIC LAMINATED PLATES

Several laminate theories, such as the classical laminate theory, the first-order shear deformation theory, and the higher-order shear deformation theory, have been proposed in the literature (see [11] for a review).

Received 21 August 2008; accepted 25 January 2010.
Address correspondence to António Ferreira, Departamento de Engenharia Mecânica e Gestão Industrial, Faculdade de Engenharia da Universidade do Portó, Rua Dr. Robertó Frias, Portó, 4200-465, Portugal. E-mail: ferreira@fe.up.pt

In the present study, the First-Order Shear Deformation Theory (FSDT) was used. This theory is based on the assumed displacement field

$$\begin{aligned} u &= u_0 + z\theta_x \\ v &= v_0 + z\theta_y \\ w &= w_0 \end{aligned} \tag{1}$$

where u and v are the in-plane displacements at any point (x, y, z) and (u_0, v_0, w_0) are the displacement components along the (x, y, z) coordinate directions, respectively, of a point on the midplane, usually considered at $z = 0$.

The transverse displacement $w(x, y)$ and the rotations $\theta_x(x, y)$ and $\theta_y(x, y)$ about the y- and x- axes are independently interpolated due to uncoupling between inplane displacements and bending displacements for symmetrically laminated plates. The equations of motion for the bending of laminated plates [11,12] are obtained as:

$$\begin{aligned} &D_{11}\frac{\partial^2\theta_x}{\partial x^2} + D_{16}\frac{\partial^2\theta_y}{\partial x^2} + (D_{12} + D_{66})\frac{\partial^2\theta_y}{\partial x\partial y} + 2D_{16}\frac{\partial^2\theta_x}{\partial x\partial y} \\ &+ D_{66}\frac{\partial^2\theta_x}{\partial y^2} + D_{26}\frac{\partial^2\theta_y}{\partial y^2} + -kA_{45}\left(\theta_y + \frac{\partial w}{\partial y}\right) \\ &- kA_{55}\left(\theta_x + \frac{\partial w}{\partial x}\right) = 0 \end{aligned} \tag{2}$$

$$\begin{aligned} &D_{16}\frac{\partial^2\theta_x}{\partial x^2} + D_{66}\frac{\partial^2\theta_y}{\partial x^2} + (D_{12} + D_{66})\frac{\partial^2\theta_x}{\partial x\partial y} + 2D_{26}\frac{\partial^2\theta_y}{\partial x\partial y} \\ &+ D_{26}\frac{\partial^2\theta_x}{\partial y^2} + D_{22}\frac{\partial^2\theta_y}{\partial y^2} + -kA_{44}\left(\theta_y + \frac{\partial w}{\partial y}\right) \\ &- kA_{45}\left(\theta_x + \frac{\partial w}{\partial x}\right) = 0 \end{aligned} \tag{3}$$

$$\begin{aligned} &\frac{\partial}{\partial x}\left[kA_{45}\left(\theta_y + \frac{\partial w}{\partial y}\right) + kA_{55}\left(\theta_x + \frac{\partial w}{\partial x}\right)\right] \\ &+ \frac{\partial}{\partial y}\left[kA_{44}\left(\theta_y + \frac{\partial w}{\partial y}\right) + kA_{45}\left(\theta_x + \frac{\partial w}{\partial x}\right)\right] = q, \end{aligned} \tag{4}$$

where q is the applied load, D_{ij} and A_{ij} are the bending and shear stiffness components, and k is the shear correction factor. Here h denotes the total thickness of the composite plate.

The bending moments M_x, M_y, and M_{xy} and the shear forces Q_x and Q_y are expressed as functions of the displacement gradients and the material stiffness components as

$$M_x = D_{11}\frac{\partial\theta_x}{\partial x} + D_{12}\frac{\partial\theta_y}{\partial y} + D_{16}\left(\frac{\partial\theta_x}{\partial y} + \frac{\partial\theta_y}{\partial x}\right) \tag{5}$$

$$M_y = D_{12}\frac{\partial\theta_x}{\partial x} + D_{22}\frac{\partial\theta_y}{\partial y} + D_{26}\left(\frac{\partial\theta_x}{\partial y} + \frac{\partial\theta_y}{\partial x}\right) \tag{6}$$

$$M_{xy} = D_{16}\frac{\partial\theta_x}{\partial x} + D_{26}\frac{\partial\theta_y}{\partial y} + D_{66}\left(\frac{\partial\theta_x}{\partial y} + \frac{\partial\theta_y}{\partial x}\right) \tag{7}$$

$$Q_x = kA_{55}\left(\theta_x + \frac{\partial w}{\partial x}\right) + kA_{45}\left(\theta_y + \frac{\partial w}{\partial y}\right) \tag{8}$$

$$Q_y = kA_{45}\left(\theta_x + \frac{\partial w}{\partial x}\right) + kA_{55}\left(\theta_y + \frac{\partial w}{\partial y}\right). \tag{9}$$

The boundary conditions for an arbitrary edge with simply supported, clamped, or free-edge conditions are defined as follows:

1. Simply supported:
   - SS1: $w = 0; M_n = 0; M_{ns} = 0.$
   - SS2: $w = 0; M_n = 0; \theta_s = 0.$
2. Clamped: $w = 0; \theta_n = 0; \theta_s = 0.$
3. Free: $Q_n = 0; M_n = 0; M_{ns} = 0.$

In previous equations, the subscripts n and s refer to the normal and tangential directions of the edge, respectively; M_n, $M_{ns,}$ and Q_n represent the normal bending moment, twisting moment and shear force on the plate edge; θ_n and θ_s represent the rotations about the tangential and normal coordinates at the plate edge. The stress resultants on an edge whose normal is represented by $\mathbf{n} = (n_x, n_y)$ can be expressed as

$$M_n = n_x^2 M_x + 2n_x n_y M_{xy} + n_y^2 M_y \tag{10}$$

$$M_{ns} = \left(n_x^2 - n_y^2\right)M_{xy} - n_x n_y (M_y - M_x) \tag{11}$$

$$Q_n = n_x Q_x + n_y Q_y \tag{12}$$

$$\theta_n = n_x\theta_x + n_y\theta_y \tag{13}$$

$$\theta_s = n_x\theta_y - n_y\theta_x, \tag{14}$$

where n_x and n_y are the direction cosines of a unit normal vector at a point at the laminated plate boundary [11,12].

Note that we can analyze Mindlin isotropic plates by considering $D_{11} = D_{22} = D = \frac{Eh^3}{12(1-\nu^2)}$, $D_{12} = \nu D_{11}$, $D_{66} = \frac{Gh^3}{12}$, $A_{55} = A_{44} = kGh$ and $D_{16} = D_{26} = A_{45} = 0$, where E is the modulus of elasticity and ν is Poisson's ratio of the isotropic material.

For further details about the FSDT, readers should consult [11].

3. THE COLLOCATION TECHNIQUE

The meshless radial basis functions method was first used by Hardy [13, 14] in the interpolation of geographical data. Later, Kansa used it for the solution of PDE [2, 3]. Nowadays this technique is well known for solving systems of PDEs with excellent accuracy [2–6].

Both Hardy and Kansa used the multiquadric radial basis function

$$g(r, c) = \sqrt{(r^2 + c^2)}; \tag{15}$$

but many other radial basis functions can be used as interpolation functions [15], such as the

$$g(r,c) = 1/\sqrt{(r^2+c^2)}; \qquad \text{inverse multiquadric}$$
$$g(r,c) = e^{-cr^2};\ c>0 \qquad \text{gaussian}$$
$$g(r) = r^2 \log r; \qquad \text{thin plate spline}$$

Radial basis functions depend on a distance r between points in a grid and may depend on a shape parameter c. Typically, r represents the Euclidean distance, but it is not necessary to be this one.

More details about the RBF meshfree method can be found in [15].

In this article, we use the multiquadric radial basis function. It depends on the Euclidean distance r and on a shape parameter c that influences the function surface shape.

3.1. Collocation with Radial Basis Functions

Consider the generic boundary value problem with a domain Ω and boundary $\partial\Omega$, and linear differential operators L and B:

$$Lu(x) = f(x),\ x \in \Omega \subset \mathbb{R}^n; \qquad Bu|_{\partial\Omega} = q. \tag{16}$$

The function **u(x)** is approximated considering N interpolation points:

$$\mathbf{u} \simeq \bar{\mathbf{u}} = \sum_{j=1}^{N} \alpha_j g_j, \tag{17}$$

where α_j are parameters to be determined. We consider a global collocation method where the linear operators L and B acting at the domain $\Omega\backslash\partial\Omega$ and at the boundary $\partial\Omega$ define a set of global equations in the form

$$\begin{pmatrix} \mathbf{L}_{ii} & \mathbf{L}_{ib} \\ \mathbf{B}_{bi} & \mathbf{B}_{bb} \end{pmatrix} \begin{pmatrix} \alpha_i \\ \alpha_b \end{pmatrix} = \begin{pmatrix} f_i \\ q_b \end{pmatrix} \quad \text{or} \quad [\mathcal{L}][\alpha] = [\lambda], \tag{18}$$

where i and b denote the domain (interior) and boundary nodes, respectively; f_i and q_b are external conditions at the domain and at the boundary. The collocation technique produces an unsymmetric (full) coefficient matrix.

The function g represents a radial basis function. In our formulation we consider the multiquadric function in the form

$$g(r,\epsilon) = \sqrt{1+(\epsilon r)^2}. \tag{19}$$

It depends on the Euclidean distance r and on a shape parameter ϵ that works as a fine tuning for better performance. This formulation is equivalent to the one in (15) if we set $\epsilon = 1/c$.

We are using different shape function ϵ for all nodes, so that:

$$g_i(r,\epsilon) = (1+(\|x-x_j\|\epsilon_i)^2)^{\frac{1}{2}}. \tag{20}$$

Applying the collocation method with N centers (boundary and interior included) and g_j defined in (20), the governing differential equations (2) to (4) are interpolated for each node as

$$\begin{aligned}
&\sum_{j=1}^{N} \alpha_j^{\theta_x} D_{11} \frac{\partial^2 g_j}{\partial x^2} + \sum_{j=1}^{N} \alpha_j^{\theta_y} D_{16} \frac{\partial^2 g_j}{\partial x^2} + \sum_{j=1}^{N} \alpha_j^{\theta_y} (D_{12}+D_{16}) \frac{\partial^2 g_j}{\partial x \partial y} \\
&\quad + 2\sum_{j=1}^{N} \alpha_j^{\theta_x} D_{16} \frac{\partial^2 g_j}{\partial x \partial y} + \sum_{j=1}^{N} \alpha_j^{\theta_x} D_{66} \frac{\partial^2 g_j}{\partial y^2} + \sum_{j=1}^{N} \alpha_j^{\theta_y} D_{26} \frac{\partial^2 g_j}{\partial y^2} \\
&\quad - k\sum_{j=1}^{N} \alpha_j^{\theta_y} A_{45} g_j - k\sum_{j=1}^{N} \alpha_j^{w} A_{45} \frac{\partial g_j}{\partial y} - k\sum_{j=1}^{N} \alpha_j^{\theta_x} A_{55} g_j \\
&\quad - k\sum_{j=1}^{N} \alpha_j^{w} A_{55} \frac{\partial g_j}{\partial x} = 0
\end{aligned} \tag{21}$$

$$\begin{aligned}
&\sum_{j=1}^{N} \alpha_j^{\theta_x} D_{16} \frac{\partial^2 g_j}{\partial x^2} + \sum_{j=1}^{N} \alpha_j^{\theta_y} D_{66} \frac{\partial^2 g_j}{\partial x^2} + \sum_{j=1}^{N} \alpha_j^{\theta_x} (D_{12}+D_{66}) \frac{\partial^2 g_j}{\partial x \partial y} \\
&\quad + 2\sum_{j=1}^{N} \alpha_j^{\theta_y} D_{26} \frac{\partial^2 g_j}{\partial x \partial y} + \sum_{j=1}^{N} \alpha_j^{\theta_x} D_{26} \frac{\partial^2 g_j}{\partial y^2} + \sum_{j=1}^{N} \alpha_j^{\theta_y} D_{22} \frac{\partial^2 g_j}{\partial y^2} \\
&\quad - k\sum_{j=1}^{N} \alpha_j^{\theta_y} A_{44} g_j - k\sum_{j=1}^{N} \alpha_j^{w} A_{44} \frac{\partial g_j}{\partial y} - k\sum_{j=1}^{N} \alpha_j^{\theta_x} A_{45} g_j \\
&\quad - k\sum_{j=1}^{N} \alpha_j^{w} A_{45} \frac{\partial g_j}{\partial x} = 0
\end{aligned} \tag{22}$$

$$\begin{aligned}
&k\sum_{j=1}^{N} \alpha_j^{\theta_y} A_{45} \frac{\partial g_j}{\partial x} + k\sum_{j=1}^{N} \alpha_j^{w} A_{45} \frac{\partial^2 g_j}{\partial x \partial y} + k\sum_{j=1}^{N} \alpha_j^{\theta_x} A_{55} \frac{\partial g_j}{\partial x} \\
&\quad + k\sum_{j=1}^{N} \alpha_j^{w} A_{55} \frac{\partial^2 g_j}{\partial x^2} + k\sum_{j=1}^{N} \alpha_j^{\theta_y} A_{44} \frac{\partial g_j}{\partial y} + k\sum_{j=1}^{N} \alpha_j^{w} A_{44} \frac{\partial^2 g_j}{\partial y^2} \\
&\quad + k\sum_{j=1}^{N} \alpha_j^{\theta_x} A_{45} \frac{\partial g_j}{\partial y} + k\sum_{j=1}^{N} \alpha_j^{w} A_{45} \frac{\partial^2 g_j}{\partial x \partial y} = q.
\end{aligned} \tag{23}$$

The vector of $3N$ unknowns α_j is composed by the α_i parameters for w_0, θ_x, and θ_y, denoted as α_j^w, $\alpha_j^{\theta_x}$, and $\alpha_j^{\theta_y}$, respectively.

Both simply supported and clamped nodes include the boundary condition $w_i = 0$, interpolated as

$$\sum_{j=1}^{N} \alpha_j^{w} g_i = 0. \tag{24}$$

Depending on the boundary condition, different equations have to be added to this one, by modifying the corresponding ith row:

1. For a clamped edge, we also impose $\theta_x = 0$ and $\theta_y = 0$ at all boundary nodes i by the following interpolation

$$\sum_{j=1}^{N} \alpha_j^{\theta_x} g_i = 0 \tag{25}$$

$$\sum_{j=1}^{N} \alpha_j^{\theta_y} g_i = 0. \tag{26}$$

2. Simply supported edge
   (a) For each node i of a simply supported edge $x = a$, we must add $M_x = 0$ and $\theta_y = 0$,

$$D_{11} \sum_{j=1}^{N} \alpha_j^{\theta_x} \frac{\partial g_i}{\partial x} + D_{12} \sum_{j=1}^{N} \alpha_j^{\theta_y} \frac{\partial g_i}{\partial y} + D_{16} \left(\sum_{j=1}^{N} \alpha_j^{\theta_x} \frac{\partial g_i}{\partial y} + \sum_{j=1}^{N} \alpha_j^{\theta_y} \frac{\partial g_i}{\partial x} \right) = 0 \tag{27}$$

$$\sum_{j=1}^{N} \alpha_j^{\theta_y} g_i = 0 \tag{28}$$

   (b) Similarly, for each node i of a simply supported edge $y = a$, we will impose $M_y = 0$ and $\theta_x = 0$,

$$D_{12} \sum_{j=1}^{N} \alpha_j^{\theta_x} \frac{\partial g_i}{\partial x} + D_{22} \sum_{j=1}^{N} \alpha_j^{\theta_y} \frac{\partial g_i}{\partial y} + D_{26} \left(\sum_{j=1}^{N} \alpha_j^{\theta_x} \frac{\partial g_i}{\partial y} + \sum_{j=1}^{N} \alpha_j^{\theta_y} \frac{\partial g_i}{\partial x} \right) = 0 \tag{29}$$

$$\sum_{j=1}^{N} \alpha_j^{\theta_x} g_i = 0. \tag{30}$$

4. THE RESIDUAL SUBSAMPLING TECHNIQUE APPLIED TO PLATES

The application of the residual subsampling technique [1] to plates can be summarized as follows.

The user prescribes first both the lower and the higher residual thresholds and the number of initial non-overlapping boxes in the domain Ω. When applied to 2D, the boxes are quadrilaterals and each box contains one RBF center and four residual points, in which the residual is evaluated. The residual points do not contribute to the RBF solution, only the RBF centers do.

Figure 1 represents four initial boxes with its centers and residual points.

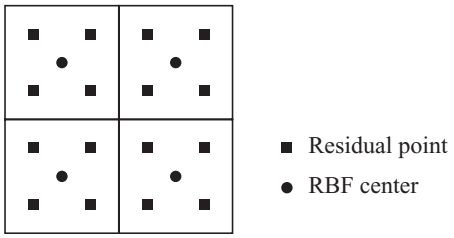

FIG. 1. Initial set of boxes, RBF centers, and residual points.

With the current set of RBF centers, we evaluate the PDE solution, as

$$L\alpha = f, \tag{31}$$

where L, f correspond to Eqs. (16)–(18).

Parameters α are then used to obtain the solution

$$A\alpha = u, \tag{32}$$

where A is the RBF interpolation matrix and u the current solution at the RBF centers (displacements w and rotations θ_x, θ_y).

At each residual point the residual is obtained by

$$Lu - f = r. \tag{33}$$

If, in each box, any residual value is larger than the higher prescribed residual tolerance, we then proceed to the next iteration with a refined set of boxes. At any box it is possible to have up to 4 new boxes. The case where we have 3 new ones is illustrated in Figure 2.

For every new box the value of the shape parameter ϵ_i (see Eq. (19)) is set double of that of its parents. Furthermore, whenever a box generates a new box the value of ϵ of the existing box is also doubled. We are somehow trying to keep the shape of the basis function constant on all scales as defined by local node spacing, since we double the shape parameter when centers become twice together.

In those boxes, wherein all residual points, the residual r is lower than the lower prescribed tolerance, RBF centers are

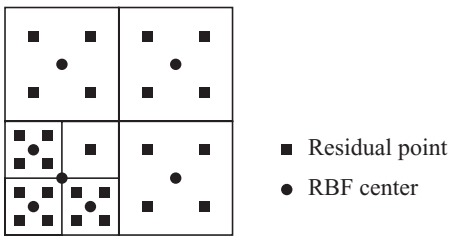

FIG. 2. Refined set of boxes, RBF centers, and residual points.

removed. In Figure 3 is illustrated the case of the four residual points associated to the RBF center located at the left and bottom having all residual smaller than the lower threshold imposed at the beginning.

If in each box all residuals meet the expected tolerance, we then remove that RBF center and proceed with a coarser grid.

For the new RBF center grid we iterate again by

- setting up a new shape parameter for each box;
- evaluating the solution $L\alpha = f$ and $A\alpha = u$; and
- controling residuals at the new residual points in each box $Lu - f = r$ and proceed as before.

5. NUMERICAL EXPERIMENTS FOR PLATES IN BENDING

We consider both isotropic and composite square plates in bending with length a and thickness h. The thickness to length ratios considered are $a/h = 10$ and $a/h = 100$.

The boundary conditions are either all edges simply-supported (SSSS) or all edges clamped (CCCC).

We consider a fixed boundary with 49 equally spaced points per side.

In the domain, we start with $N = 4$ (corresponding to $4^2 = 16$ boxes) or $N = 5$ (corresponding to $5^2 = 25$ boxes), being these quite coarse grids.

In Figure 4 the initial centers and residual points considered are presented for $N = 4$ and $N = 5$. When the chosen N is even, we introduce the plate central point as a center, without considering any checkbox or residual ckeckpoint. This was done to make possible the comparison with the exact solution as we always compare results by this adaptive method with analytical solutions obtained by series solutions. Errors are expressed in %.

The initial shape parameter is $\epsilon = 2/N$ for each center box, corresponding to $\epsilon = 2/4$ or $\epsilon = 2/5$. The chosen higher residual tolerance is $5*10^{-4}$ and the lower one is $5*10^{-7}$.

When applying the RBF collocation technique, the same set of points is usually used for centers and interpolation (collocation). In the present study that was done at the step of the algorithm where we obtain α by solving Eq. (31). However, at the step of the algorithm where the residual is evaluated by Eq. (33), the boxes centers were the collocation points and the residual points were the boxes centers and so matrix L in (33) has dimension $3N * 3M$, being N the total number of centers (center boxes and boundary points) and M the number of residual points.

The process stops when there are no more points to be added.

TABLE 1
Isotropic square plate SSSS, $a/h = 10$, 16 initial boxes.

Centers	Error (%)	Adds
209	1.077958e + 000	64
273	4.654796e − 001	63
336	7.690783e − 001	9
345	7.477775e − 001	2
347	7.407987e − 001	2
349	7.634622e − 001	0

TABLE 2
Isotropic square plate SSSS, $a/h = 10$, 25 initial boxes.

Centers	Eerror (%)	Adds
217	3.545147e + 000	100
317	7.549590e − 001	5
322	7.601606e − 001	0

5.1. Isotropic Plates

In this subsection, we consider an isotropic plate with modulus of elasticity $E = 10,920$ and Poisson's coefficient $\nu = 0.25$. The non-dimensional transverse displacement is given by

$$\overline{w} = 10^2 \frac{E_2 h^3}{a^4} w \tag{34}$$

for every solution.

In the following tables, we present the number of centers, the relative error in percentage, and the number of centers to be added at each iteration for the different isotropic plates analyzed. In all performed tests, there are no points to be removed.

In Tables 1 and 2 we present the evolution of the method for the isotropic square plate in bending, with thickness to length ratio $a/h = 10$, and simply-supported (SSSS) boundary condition. In Table 1 we show results with 16 initial boxes and in Table 2 we show results with 25 initial boxes. The analytical solution obtained by Lévy series solutions for this case is 4.7543.

In Figure 3 the centers and the boxes at the third iteration are presented for the isotropic square plate in bending, with thickness to length ratio $a/h = 10$, simply-supported, and starting with 16 boxes. In Figure 6 we present the final centers and the deformed shape for the same case.

The final RBF centers and deformed shape of the isotropic square plate in bending, with thickness to length ratio $a/h = 10$, simply supported, starting with 25 boxes are shown in Figure 7.

In Table 3 is possible to see the evolution of the iterative method when applied to the isotropic simply supported

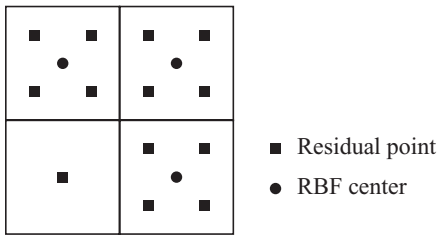

FIG. 3. Coarse set of RBF centers.

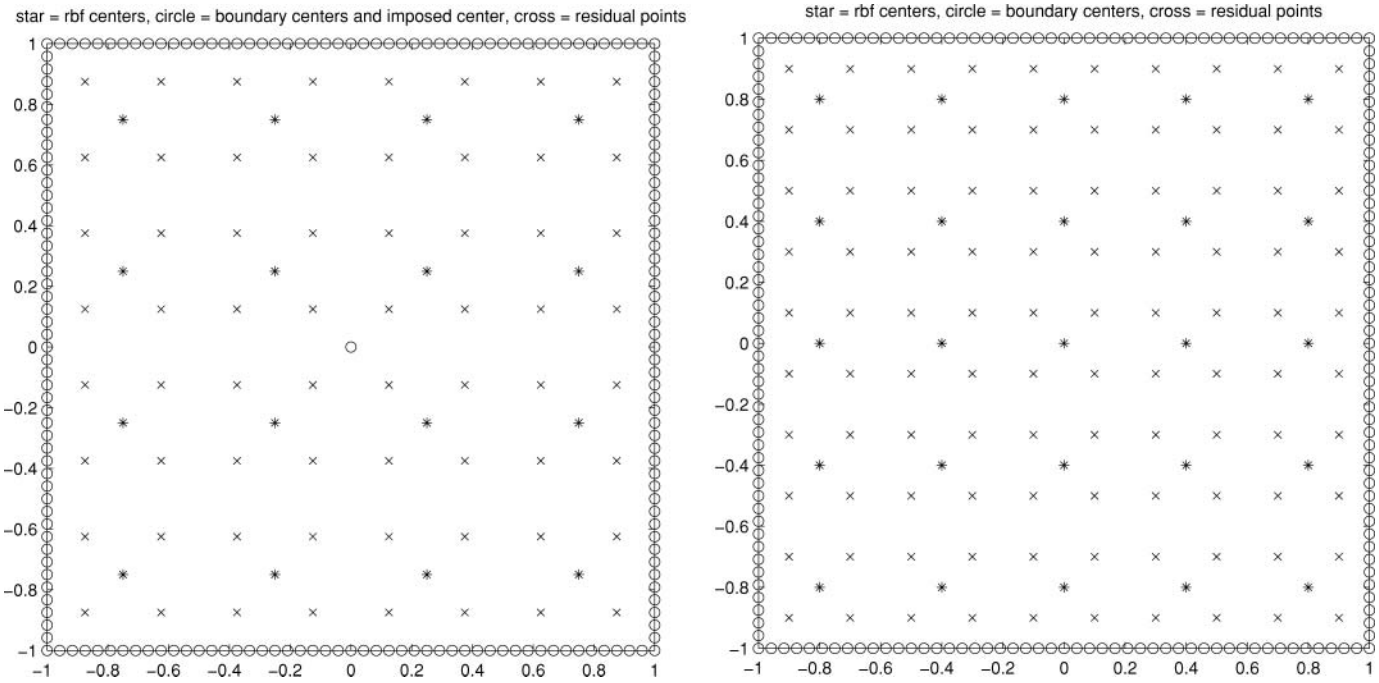

FIG. 4. Initial boxes for $N = 4$ (on the left) and $N = 5$ (on the right).

square plate, with thickness to length ratio $a/h = 100$, in bending, starting with 16 boxes. Results for the same plate but using 25 initial boxes are shown in Table 4. The analytical solution obtained by Lévy series solutions for this case is 4.5720.

The final set of RBF centers of the isotropic simply supported square plate in bending, with thickness to length ratio $a/h = 100$ are shown in Figure 8. On the left the case of 16 initial boxes is illustrated, and on the right the case of 25 initial boxes is illustrated.

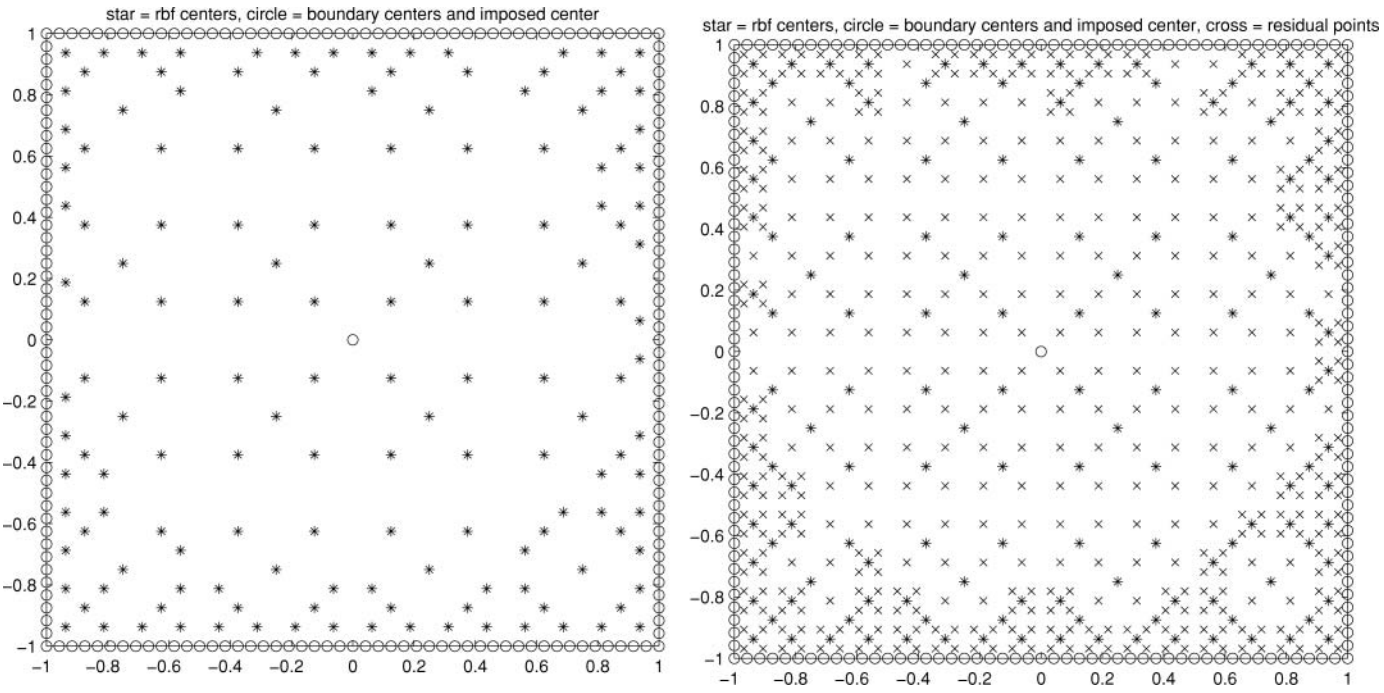

FIG. 5. Distribution of centers (left) and boxes (right) at third iteration, isotropic square plate, SSSS, $a/h = 10$, 16 initial boxes.

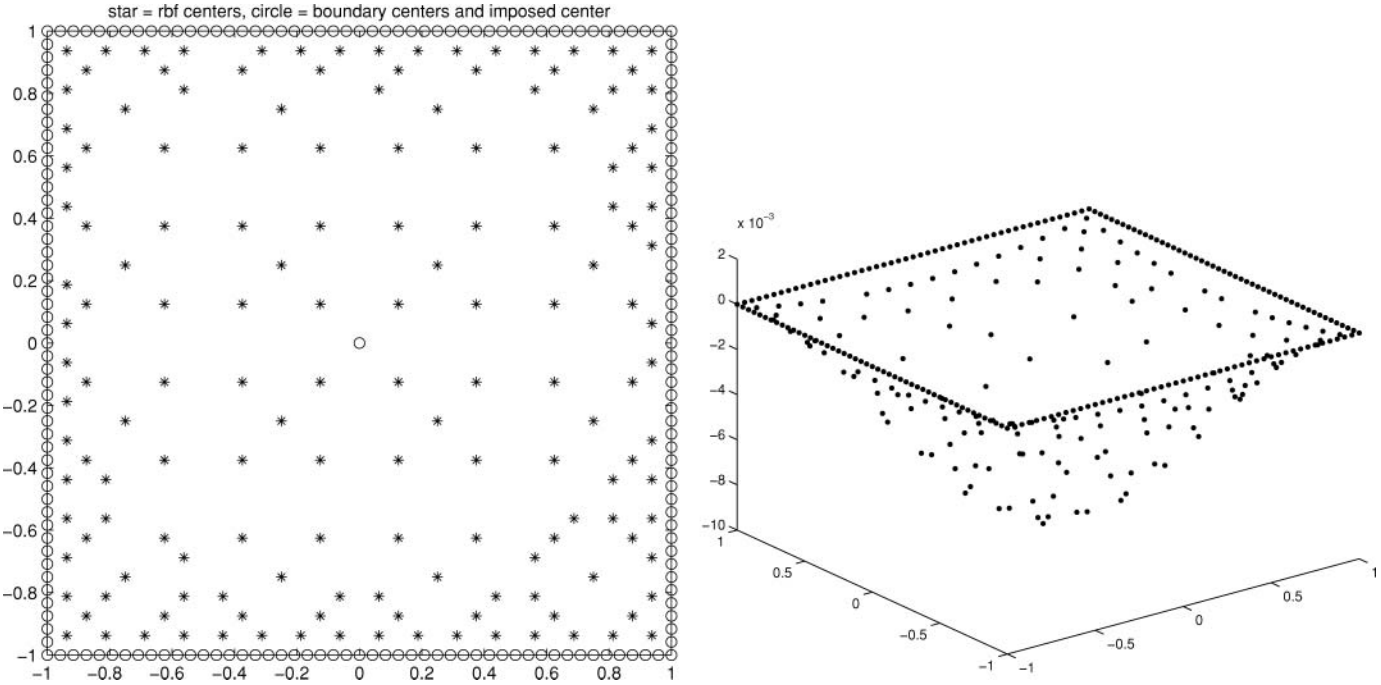

FIG. 6. Final centers and deformed shape of isotropic square plate, SSSS, $a/h = 10$, 16 initial boxes.

TABLE 3
Isotropic square plate SSSS, $a/h = 100$, 16 initial boxes.

Centers	Error (%)	Adds
209	9.999748e + 001	64
273	3.417590e + 000	168
441	5.100564e − 001	175
616	1.198528e − 002	25
641	5.794928e − 002	0

TABLE 4
Isotropic square plate SSSS, $a/h = 100$, 25 initial boxes.

Centers	Error (%)	Adds
217	1.728831e + 001	100
317	1.162787e + 000	141
458	7.501994e − 002	16
474	2.619898e − 002	19
493	5.042478e − 002	6
499	1.589558e − 002	2
501	5.990400e − 002	5
506	3.266486e − 002	2
508	3.155965e − 002	8
516	2.367293e − 002	1
517	1.635045e − 002	1
518	2.050627e − 002	0

5.2. Composite Plates

The examples considered here are limited to symmetric cross-ply laminates with layers of equal thickness and with identical material properties. The composite plates laminates are [0/90/0] (having 3 layers, each one with thickness $h/3$), and [0/90/90/0] (denoted as $[0/90]_s$ and having 4 layers, each one with thickness $h/4$).

The material properties are

$$E_1 = 25E_2;\ G_{23} = 0.2E_2;\ G_{12} = G_{13} = 0.5E_2;$$
$$\nu_{12} = 0.25;\ \nu_{21} = \nu_{12}\frac{E_2}{E_1}$$

As in the isotropic case, the tables below illustrate the evolution of the entire process of the iterative technique applied to the bending analysis of plates with respect to the number of RBF centers, the percentual relative error, and the number of centers to be added at each iteration. Once again, there are no points to be removed in all studied cases.

We use the same non-dimensional factor as in Eq. (34).

Tables 5 (16 initial boxes) and 6 (25 initial boxes) refer to the case of the composite [0/90/0] square plate in bending, with thickness to length ratio $a/h = 10$, and simply-supported (SSSS) boundary condition. The error is obtained by comparing with Mindlin solution [16], $\bar{w} = 1.0211$.

The set of RBF centers at the end of the iterative process of the [0/90/0] simply-supported square plate in bending, with thickness to length ratio $a/h = 10$ are presented in Figure 7.

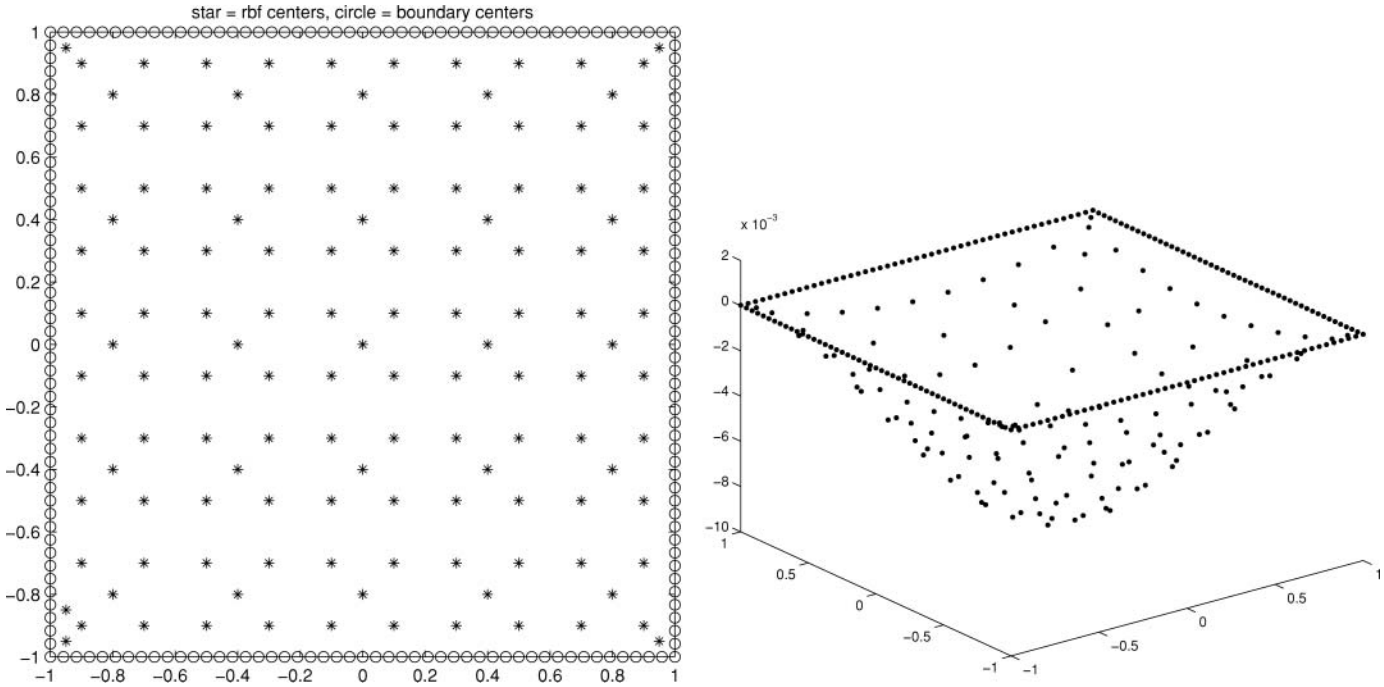

FIG. 7. Final centers and deformed shape of isotropic square plate, SSSS, $a/h = 10$, 25 initial boxes.

TABLE 5
[0/90/0] square plate SSSS, $a/h = 10$, 16 initial boxes.

Centers	Error (%)	Adds
209	1.654938e + 000	64
273	5.681379e − 002	33
306	2.037581e − 001	70
376	3.746343e − 001	78
454	1.127763e − 001	23
477	1.680405e − 001	4
481	3.267953e − 001	3
484	9.192459e − 002	4
488	5.203128e − 002	2
490	1.329159e − 001	0

TABLE 6
[0/90/0] square plate SSSS, $a/h = 10$, 25 initial boxes.

Centers	Error (%)	Adds
217	2.534830e+000	98
315	1.683086e − 001	31
346	1.696108e − 001	21
367	1.790651e − 001	1
368	1.612302e − 001	0

On the left we show the case of 16 initial boxes and on the right the case of 25 initial boxes.

Table 7 illustrates the iterative process results for laminated [0/90/0] simply supported square plate in bending, with $a/h = 100$ and 16 initial boxes. Table 8 presents results for the same problem, but with 25 initial boxes. Error is obtained by comparing the solution with the Mindlin solution [16], $\bar{w} = 0.6701$.

Table 9 illustrates the iterative process results for laminated [0/90/0] clamped square plate in bending, with $a/h = 10$ and 16 initial boxes. Table 10 presents results for the same problem, but with 25 initial boxes. Error is obtained by comparing the solution with the Mindlin solution [16], $\bar{w} = 0.4829$.

Table 11 illustrates the iterative process results for laminated $[0/90]_s$ simply supported square plate in bending, with $a/h = 10$ and 16 initial boxes. Table 12 presents results for the same

TABLE 7
[0/90/0] square plate SSSS, $a/h = 100$, 16 initial boxes.

Centers	Error (%)	Adds
209	3.619099e + 000	64
273	7.461579e − 001	170
443	1.243793e + 000	125
568	1.816361e − 001	50
618	5.638896e − 002	15
633	1.571762e − 001	4
637	1.110252e − 001	0

TABLE 8
[0/90/0] square plate SSSS, $a/h = 100$, 25 initial boxes.

Centers	Error (%)	Adds
217	9.756506e + 000	100
317	2.809135e − 001	71
388	1.355320e − 001	27
415	2.087332e − 001	20
435	2.012888e − 001	19
454	1.142907e − 001	11
465	1.947379e − 001	28
493	2.773958e − 001	16
509	1.792259e − 001	5
514	2.683916e − 001	6
520	2.199761e − 001	0

TABLE 9
[0/90/0] square plate CCCC, $a/h = 10$, 16 initial boxes.

Centers	Error (%)	Adds
209	1.882287e + 000	60
269	4.101527e − 001	60
329	3.416589e − 002	41
370	2.623125e − 001	86
456	4.951293e − 001	28
484	6.473929e − 002	8
492	1.792660e − 002	24
516	1.677414e − 002	11
527	2.957150e − 002	2
529	4.054957e − 003	2
531	1.841740e − 002	2
533	1.273115e − 002	4
537	8.016174e − 003	0

problem, but with 25 initial boxes. Error is obtained by comparing the solution with the Navier solution [11], $\bar{w} = 1.0250$.

Table 13 illustrates the iterative process results for laminated $[0/90]_s$ simply supported square plate in bending, with $a/h = 100$ and 16 initial boxes. Table 14 presents results for the same problem, but with 25 initial boxes. Error is obtained by comparing the solution with the Navier solution [11], $\bar{w} = 0.6833$.

TABLE 10
[0/90/0] square plate CCCC, $a/h = 10$, 25 initial boxes.

Centers	Error (%)	Adds
217	1.810916e − 001	100
317	7.859572e − 003	31
348	2.139349e − 002	28
376	6.628577e − 003	2
378	2.498585e − 002	10
388	1.358878e − 002	0

5.3. Discussion of Results

On the numerical examples presented, the number of iterations varies from 3 to 13. In every case the error is inferior to 1% after a few iterations. This is a very satisfactory result.

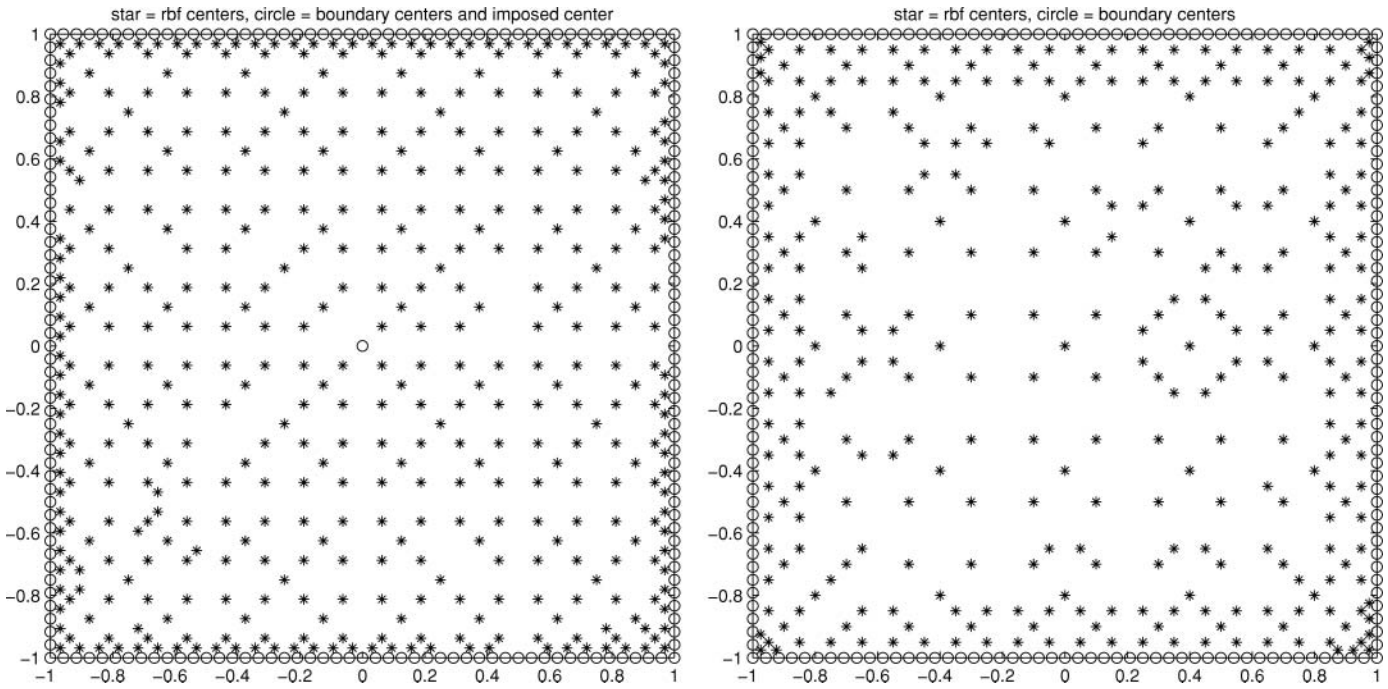

FIG. 8. Final centers of the isotropic square plate, SSSS, $a/h = 100$, 16 (left) and 25 (right) initial boxes.

TABLE 11
$[0/90]_s$ square plate SSSS, $a/h = 10$, 16 initial boxes.

Centers	Error (%)	Adds
401	1.556392e + 000	64
465	2.962116e − 001	68
533	1.578955e − 001	75
608	4.448880e − 001	48
656	2.274114e − 001	18
674	9.422296e − 002	8
682	1.123366e − 001	7
689	1.659383e − 001	10
699	2.400472e − 001	3
702	2.035321e − 001	3
705	2.367390e − 001	6
711	2.533541e − 001	0

TABLE 12
$[0/90]_s$ square plate SSSS, $a/h = 10$, 25 initial boxes.

Centers	Error (%)	Adds
409	2.607549e + 000	97
506	2.909581e − 001	37
543	2.425400e − 001	15
558	2.032778e − 001	11
569	2.095007e − 001	0

TABLE 13
$[0/90]_s$ square plate SSSS, $a/h = 100$, 16 initial boxes.

Centers	Error (%)	Adds
401	1.158316e + 001	64
465	6.423911e − 001	155
620	2.633451e + 000	131
751	1.097797e − 001	74
825	2.712160e − 001	1
826	2.015782e − 001	3
829	2.789185e − 001	0

TABLE 14
$[0/90]_s$ square plate SSSS, $a/h = 100$, 25 initial boxes.

Centers	Error (%)	Adds
409	9.781134e + 000	100
509	6.547123e − 001	86
595	2.146976e − 001	9
604	4.799680e − 001	30
634	3.497355e − 001	15
649	3.209971e − 001	16
665	3.653390e − 001	7
672	3.684787e − 001	0

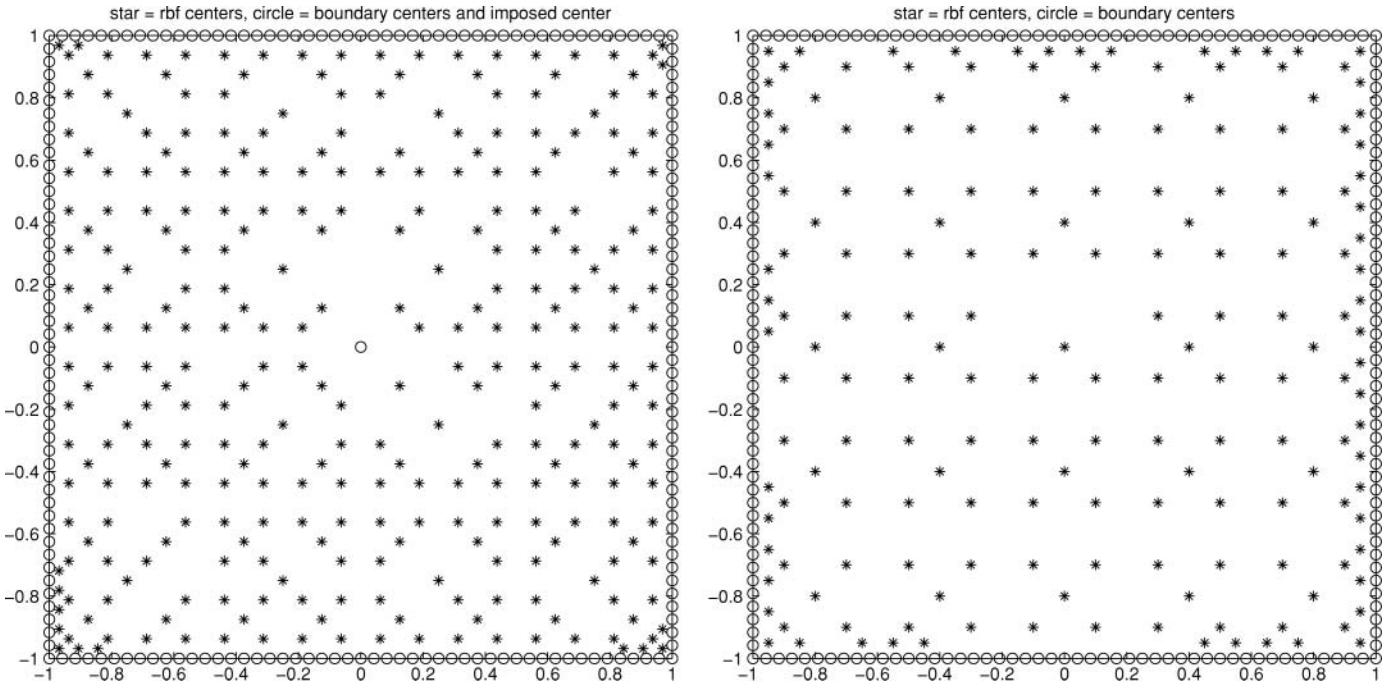

FIG. 9. Final centers of the [0/90/0] square plate, SSSS, $a/h = 10$, 16 (left) and 25 (right) initial boxes.

Taking in to consideration the number of initial boxes, two remarks are to be made. At the end of the iterative process, we always obtain more points if we start with 16 boxes, but it doesn't seem to have any influence in the number of iterations.

Thin plates generate more points than thick plates. The clamped case needs more points than the simply supported case.

At the end of each iteration process, the cloud of points is more dense near the boundary than in the central zone of the plate.

The process used to find α from equation $L\alpha = f$ is determinant for the performance of the process. The GMRES method is less sensitive to the shape parameter ϵ than the backslash Matlab operator \ and it has influence on the number of centers to add and remove and, consequently, in the number of final RBF centers. The backslash Matlab operator generates more points and the deformed plate frequently degenerates. Using the GMRES Matlab command, the deformed is more stable from the beginning till the end of the iterative process, but it is much more time consuming. This can be explained with the computational cost and the storage requirements that, according to [17], increases linearly with the number of iterations.

6. CONCLUSION

This article addresses the adaptive static analysis of isotropic and composite plates with radial basis multiquadric functions.

The residual subsampling technique proposed by Driscoll and Heryudono [1] was used for the domain with a fixed boundary grid.

Numerical tests were then performed on the bending analysis of isotropic and symmetric cross-ply laminated square plates. A first-order shear deformation theory was used. When applying the Driscoll and Heryudono residual subsampling technique to bending analysis, the residual has to be improved to take in to consideration the degrees of freedom, three in this case.

In this technique, the user must prescribe the residual tolerance, the initial number of nodes, and the initial shape parameter. This parameter is then modified for each nodal box in order to control the conditioning of the coefficient matrix.

We calculate the error of the present method with respect to the exact solutions. The results obtained show that the adaptive method converges to a very good solution after a few iterations even by starting with a very coarse grid.

Further studies, including optimization of the shape parameter in each iteration, are sought. The combination of optimization techniques with adaptive methods may reduce the number of nodes in each iteration. The present method may generate quite a large number of nodes, depending on the thickness of the plate, and the way we select the shape parameters.

REFERENCES

1. T.A. Driscoll, and A.R.H. Heryudono, Adaptive Residual Subsampling Methods for Radial Basis Function Interpolation and Collocation Problems, Comput. & Math. Appl., vol. 53, no. 6, pp. 927–939, 2007.
2. E.J. Kansa, Multiquadrics. A Scattered Data Approximation Scheme with Applications to Computational Fluid-dynamics. I. Surface Approximations and Partial Derivative Estimates, Comput. & Math. Appl., vol. 19, no. (8–9), pp. 127–145, 1990.
3. E.J. Kansa, Multiquadrics. A Scattered Data Approximation Scheme with Applications to Computational Fluid-dynamics. II. Solutions to Parabolic, Hyperbolic and Elliptic Partial Differential Equations, Comput. & Math. Appl., vol. 19, no. (8–9), pp. 147–161, 1990.
4. E. Larsson, and B. Fornberg, A Numerical Study of Some Radial Basis Function Based Solution Methods for Elliptic PDEs, Comput. & Math. Appl., vol. 46, no. (5–6), pp. 891–902, 2003.
5. G.E. Fasshauer, Solving Partial Differential Equations by Collocation with Radial Basis Functions, Surface Fitting and Multiresolution Methods, vol. 2. Proceedings of the 3rd International Conference on Curves and Surfaces, vol. 2, pp. 131–138, 1997.
6. S.A. Sarra, Adaptive Radial Basis Function Methods for Time Dependent Partial Differential Equations, Appl. Numer. Math., vol. 54, no. 11, pp. 79–94, 2005.
7. A.H.-D. Cheng, M.A. Golberg, E.J. Kansa, and G. Zammito, Exponential Convergence and H-c Multiquadric Collocation Method for Partial Differential Equations, Numer Methods Partial Differential Eq. 19: 571594, 2003.
8. A.J.M. Ferreira, C.M.C. Roque, and P.A.L.S. Martins, Analysis of Composite Plates Using Higher-Order Shear Deformation Theory and a Finite Point Formulation Based on the Multiquadric Radial Basis Function Method, Composites Part B: Engineering, vol. 34, pp. 627–636, 2003.
9. A.J.M. Ferreira, Polyharmonic (Thin-Plate) Splines in the Analysis of Composite Plates, Int. J. Mech. Sci., vol. 46, no. 10, pp. 1549–1569, 2004.
10. A.J.M. Ferreira, C.M.C. Roque, and P.A.L.S. Martins, Radial Basis Functions and Higher-Order Theories in the Analysis of Laminated Composite Beams and Plates, Composite Struct., Vol. 66, pp. 287–293, 2004.
11. J.N. Reddy, Mechanics of Laminated Composite Plates. CRC Press, New York, 1997.
12. K.M. Liew, Y.Q. Huang, and J.N. Reddy, Vibration Analysis of Symmetrically Laminated Plates Based on FSDT Using the Moving Least Squares Differential Quadrature Method, Comp. Meth. Appl. Mech. Eng., vol. 192, pp. 2203–2222, 2003.
13. R.L. Hardy, Multiquadrics Equations of Topography and Other Irregular Surfaces, J. Geophys. Res., vol. 176, no. (8–9), pp. 1905–1915, 1971.
14. R.L. Hardy, Theory and Apllications of the Multiquadric-Biharmonic Method: 20 years of Discovery, Comput. Math. Appl., vol. 19, no. (8–9), pp. 163–208, 1990.
15. G.L. Liu, Mesh Free Methods: Moving Beyond the Finite Element Method. Boca Raton, FL: CRC Press, 2003.
16. B.N. Pandya, and T. Kant, Flexural Analysis of Laminated Composites Using Refined Higher-Order C^0 Plate Bending Elements, Comput. Methods Appl. Mech. Eng., vol. 66, pp. 173–198, 1988.
17. B. Bradie, A Friendly Introduction to Numerical Analysis. Pearson Prentice Hall, Upper Saddle River, NJ, 2006.